

SCIENTIFIC REPORTS



OPEN

Rearrangement of MICU₁ multimers for activation of MCU is solely controlled by cytosolic Ca²⁺

Received: 30 March 2015
Accepted: 07 September 2015
Published: 22 October 2015

Markus Waldeck-Weiermair*, Roland Malli*, Warisara Parichatikanond*, Benjamin Gottschalk, Corina T. Madreiter-Sokolowski, Christiane Klec, Rene Rost & Wolfgang F. Graier

Mitochondrial Ca²⁺ uptake is a vital process that controls distinct cell and organelle functions. Mitochondrial calcium uptake 1 (MICU₁) was identified as key regulator of the mitochondrial Ca²⁺ uniporter (MCU) that together with the essential MCU regulator (EMRE) forms the mitochondrial Ca²⁺ channel. However, mechanisms by which MICU₁ controls MCU/EMRE activity to tune mitochondrial Ca²⁺ signals remain ambiguous. Here we established a live-cell FRET approach and demonstrate that elevations of cytosolic Ca²⁺ rearranges MICU₁ multimers with an EC₅₀ of 4–4 μM, resulting in activation of mitochondrial Ca²⁺ uptake. MICU₁ rearrangement essentially requires the EF-hand motifs and strictly correlates with the shape of cytosolic Ca²⁺ rises. We further show that rearrangements of MICU₁ multimers were independent of matrix Ca²⁺ concentration, mitochondrial membrane potential, and expression levels of MCU and EMRE. Our experiments provide novel details about how MCU/EMRE is regulated by MICU₁ and an original approach to investigate MCU/EMRE activation in intact cells.

Mitochondrial Ca²⁺ uptake stimulates mitochondrial dehydrogenases and, thus, oxidative phosphorylation, that, ultimately results in increased ATP formation^{1,2}. Due to the effective mitochondrial Ca²⁺ buffer capacity local and global Ca²⁺ signals are shaped by mitochondria, thus, these organelles control multiple Ca²⁺-sensitive cell signaling pathways and functions³. However, mitochondrial Ca²⁺ overload is associated with an increased generation of reactive oxygen species, cell dysfunctions and the induction of cell death pathways⁴.

While the phenomenon of mitochondrial membrane potential-dependent Ca²⁺ uniport is known since the early 1960ties, the identity of key protagonists that actually accomplish and directly regulate mitochondrial Ca²⁺ uptake remained elusive until very recently. In 2011 a 35-kDa protein, which was initially referred to as CCDC109A and then renamed mitochondrial Ca²⁺ uniporter (MCU) was described to show many if not all of the typical characteristics of a Ca²⁺ uniporter^{5,6}. It has been suggested that MCU, which possesses two transmembrane domains, forms tetrameric highly specific mitochondrial Ca²⁺ channels. Interestingly, these MCU oligomers are part of larger protein complexes of the inner mitochondrial membrane, indicating the existence of complex mitochondrial Ca²⁺ uptake machineries that include other regulatory subunits⁷. While mitochondrial calcium uniporter regulator 1 (MCUR1)⁸, leucine zipper/EF hand-containing transmembrane-1 (Letm1)^{9–11} and the novel uncoupling proteins 2 and 3 (UCP2/3)^{12–14}, which have been shown to contribute to certain modes of mitochondrial Ca²⁺ uptake, have not been found in MCU containing protein complexes⁵, other types of proteins have been identified and characterized as regulatory components of the MCU machinery. These proteins include the dominant-negative pore-forming subunit MCUB¹⁵, the essential MCU regulator (EMRE)¹⁶, mitochondrial calcium uptake 1 (MICU1)^{17,18} and its isoforms^{19,20}. MICU1, which was identified some months

Institute of Molecular Biology and Biochemistry, Center of Molecular Medicine, Medical University of Graz, Harrachgasse 21/III, 8010 Graz, Austria. *These authors contributed equally to this work. Correspondence and requests for materials should be addressed to W.F.G. (email: wolfgang.graier@medunigraz.at)

earlier than MCU, has two classical EF-hand Ca^{2+} -binding domains and forms large complexes of app. 480 kDa^{17,20}. The interaction of MICU1 with MCU is mediated by EMRE^{16,21}. The two Ca^{2+} -binding EF-hand domains of MICU1 can undergo large conformational changes upon binding of Ca^{2+} ^{22,23} and face the intermembrane space¹⁸. MICU1 is a gatekeeper of MCU preventing an increase of the mitochondrial Ca^{2+} concentration ($[\text{Ca}^{2+}]_{\text{mito}}$) at low resting Ca^{2+} levels while it is thought to facilitate mitochondrial Ca^{2+} uptake upon high Ca^{2+} concentrations^{18,24,25}. Recently, an elegant study determined the crystal structure of MICU1 indicating that in the absence of Ca^{2+} MICU1 exists as a hexamer, while Ca^{2+} binding to the two EF-hands results in a rearrangement to MICU1 dimers²³. This study provided the first insights into the molecular mechanism by which MICU1 possibly controls MCU/EMRE activity and suggests that the hexameric MICU1 prevents MCU/EMRE Ca^{2+} channel activity that gets released upon (re-)organization of MICU1 hexamers/multimers⁷. However, whether or not Ca^{2+} -dependent rearrangements of MICU1 multimers indeed occur and regulate the activity of MCU in intact cells, and the impact of MCU and EMRE to the structural (re-)organization of MICU1 have not been investigated so far. Hence, the kinetics of the rearrangement of the MICU1 multimers upon cytosolic Ca^{2+} elevation and whether or not the mitochondrial matrix Ca^{2+} concentration or membrane potential (ψ_{mito}) have an impact on the structural reorganization of MICU1 remain elusive.

In this study we used a FRET-based live-cell imaging approach to dynamically monitor the kinetics of the structural (re-)organization of MICU1 and to explore its dependence from cytosolic and mitochondrial Ca^{2+} signals as well as ψ_{mito} . Simultaneous measurements of cytosolic Ca^{2+} with either mitochondrial Ca^{2+} signals or MICU1 rearrangement were performed to verify whether MICU1 multimers indeed retard MCU activation in intact cells. Finally, we tested whether the Ca^{2+} -sensitive rearrangement of MICU1 is dependent of the expression level of MCU and EMRE. Our data provide new insights in the dynamics, regulation, and molecular effect of the structural (re-)organization of MICU1 that adds to our current understanding of the complex molecular mechanisms of MCU activation.

Results

Ca^{2+} elevations yield rearrangement of MICU1 multimers in intact cells. In order to dynamically monitor whether and, if so, how intracellular Ca^{2+} -mobilization by an inositol 1,4,5-trisphosphate (IP_3 -)generating agonist affects the arrangement of MICU1 in intact cells, Förster energy transfer (FRET) imaging was applied in cells co-expressing MICU1 fused to either cyan fluorescent protein (MICU1-CFP) or yellow fluorescent protein (MICU1-YFP). Because MICU1 has been shown to assemble in hexamers in the absence of Ca^{2+} and rearranges to dimers upon Ca^{2+} binding²³, we assumed that under resting conditions the expressed MICU1-CFP and MICU1-YFP chimeras exist as hexamers, thus, facilitating FRET from CFPs to YFPs (Fig. 1A). However, elevation of Ca^{2+} and its subsequent binding to MICU1 should yield disaggregation of MICU1 hexamers and reduce the inter-MICU1 FRET signal. Indeed, cell treatment with the IP_3 -generating agonist histamine¹¹ considerably reduced the inter-MICU1 FRET ratio (Fig. 1B,C), while the agonist had no effect on fluorescence of cells expressing MICU1-YFP alone (Supplementary Fig. 1). Upon removal of the agonist the signal was restored (Fig. 1B,C), indicating the reassembly of MICU1 to higher multimers upon the decline of Ca^{2+} levels. In the nominal absence of extracellular Ca^{2+} , the histamine-triggered decrease of inter-MICU1 FRET was more transient and slowly developed upon subsequent addition of extracellular Ca^{2+} (Supplementary Fig. 2), thus, highlighting that inter-MICU1 FRET strictly follows cellular Ca^{2+} signals under these conditions (Supplementary Fig. 3). In contrast to the fast intracellular Ca^{2+} mobilization in response to histamine, slow Ca^{2+} mobilization from the endoplasmic reticulum (ER) by the sarcoplasmic/endoplasmic reticulum Ca^{2+} ATPase (SERCA) inhibitor 2,5-di-tert-butylhydroquinone (BHQ)²⁶ only slowly and weakly reduced the inter-MICU1 FRET signal (Supplementary Fig. 4). Under this condition mitochondrial Ca^{2+} uptake in response to cell treatment with BHQ was largely increased in cells treated with the 3' UTR siRNA against MICU1 (Supplementary Fig. 5), despite an almost unaffected cytosolic Ca^{2+} elevation (Supplementary Fig. 6). These findings indicate that the slow and weak ER depletion with BHQ yields only in insufficient MICU1-rearrangement, while the inhibitory function of MICU1 multimers on MCU remains under these conditions. However, expression of FP tagged MICU1 completely restored the inhibition of mitochondrial Ca^{2+} uptake at low Ca^{2+} (Supplementary Fig. 5). In contrast, using a MICU1 variant mutated in both canonical EF hands^{17,23} was neither able to rescue this siRNA mediated effect of MICU1 (Supplementary Fig. 7) nor showed any MICU1 FRET rearrangement upon stimulation with histamine (Supplementary Fig. 8).

In order to determine the affinity of the MICU1 multimers for Ca^{2+} to evoke their rearrangement *in situ*, the Ca^{2+} ionophore ionomycin was used to clamp different cytosolic Ca^{2+} concentrations (Fig. 1D,E). These experiments revealed a half maximal effective Ca^{2+} concentration (EC_{50}) to trigger rearrangement of the MICU1 multimers of 4.4 (3.7–5.2) μM in HeLa cells (Fig. 1E). Our findings are in line with studies demonstrating the existence of Ca^{2+} micro-domains of up to 16 μM in hot spots between the ER and mitochondria in response to an IP_3 -generating agonist²⁷. Such Ca^{2+} hot spots would efficiently destruct MICU1 multimers and, hence, activate mitochondrial Ca^{2+} uniport. Our results provide a first demonstration that MICU1 oligomerization is reversibly controlled by high and low $[\text{Ca}^{2+}]_{\text{cyto}}$ in intact cells.

Ca^{2+} -triggered MICU1 de-multimerization occurs prior to mitochondrial Ca^{2+} uptake. Simultaneous imaging of cytosolic and mitochondrial Ca^{2+} signals in individual single cells using a

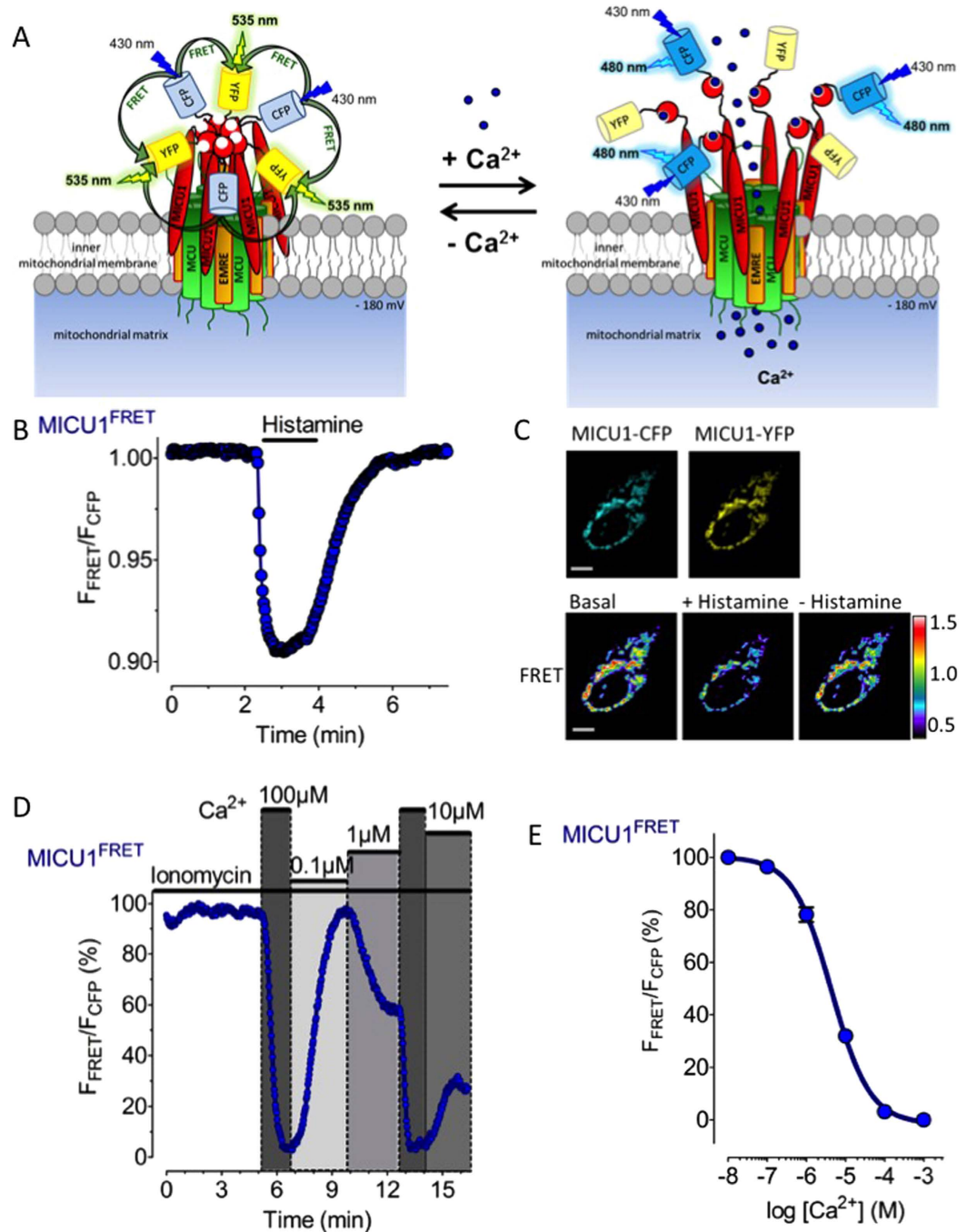


Figure 1. Ca^{2+} dynamically controls rearrangement of MICU1 multimers in intact cells. **(A)** Schematic illustration of the putative Ca^{2+} -induced rearrangement of MICU1-CFP and MICU1-YFP hexamers that bind to the MCU/EMRE mitochondrial Ca^{2+} uptake machinery. It is hypothesized that Ca^{2+} binding to the MICU1 EF-hands reduces FRET between the respective MICU1-conjugated FPs. **(B)** Representative curve showing the MICU1 FRET ratio signal of HeLa cells co-expressing MICU1-CFP and MICU1-YFP upon cell treatment with $100\ \mu\text{M}$ histamine in the presence of $2\ \text{mM}$ Ca^{2+} . **(C)** Representative images to panel b under basal condition, upon stimulation with $100\ \mu\text{M}$ histamine 3 min. after stimulation (scale bar, $10\ \mu\text{m}$). **(D)** Representative MICU1 FRET ratio signals over time in HeLa cells upon addition and removal of different free Ca^{2+} concentrations in the presence of $3\ \mu\text{M}$ ionomycin. The maximal Δ MICU1 FRET ratio signal (between $3\ \text{mM}$ EGTA and $1000\ \mu\text{M}$ Ca^{2+}) was defined as 100%. **(E)** Concentration response curve of the Ca^{2+} -induced reduction of the MICU1 FRET ratio signal in HeLa cells that were treated with $3\ \mu\text{M}$ ionomycin and different Ca^{2+} concentrations as shown in panel (D); mean \pm SEM. ($n = 7-9$).

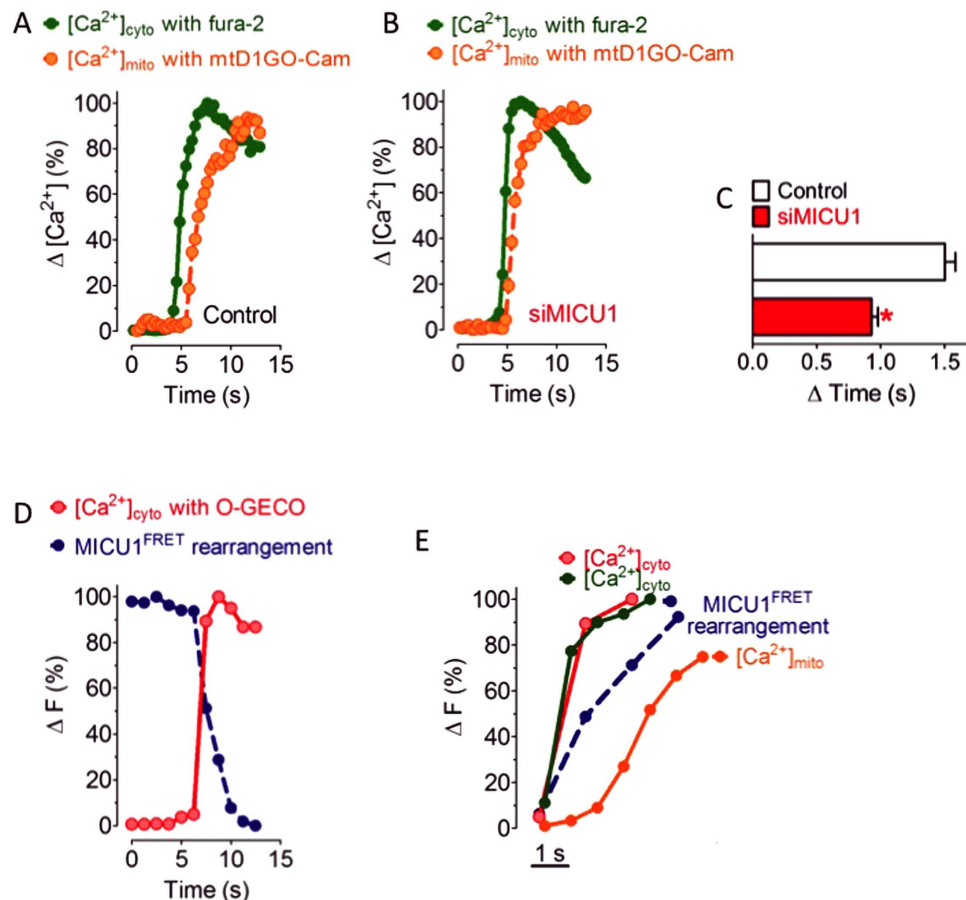


Figure 2. Rearrangement of MICU1 multimers occurs prior to mitochondrial Ca^{2+} uptake. (A, B) Fura-2/AM loaded cells expressing 4mtD1GO-Cam were used to simultaneously record $[Ca^{2+}]_{cyto}$ (green traces) and $[Ca^{2+}]_{mito}$ (orange traces) in response to cell treatment with 100 μ M histamine in the absence of extracellular Ca^{2+} in control HeLa cells (A) and cells reduced of MICU1 (B). The respective Δ ratio values were defined as 100%. (C) Bar graph showing Δ mean time values \pm SEM. between the onset of cytosolic and mitochondrial Ca^{2+} signals in response to 100 μ M histamine of individual control HeLa cells (white column, n = 7) and cells diminished of MICU1 (red column, n = 9). *P < 0.05 vs. control. (D) Representative simultaneous recording of $[Ca^{2+}]_{cyto}$ and MICU1 FRET in response to 100 μ M histamine under Ca^{2+} -free conditions using HeLa cells co-expressing O-GECO, MICU1-CFP and MICU1-YFP. (E) Temporal correlation of $[Ca^{2+}]_{cyto}$, $[Ca^{2+}]_{mito}$ and MICU1 FRET in response to cell treatment with 100 μ M histamine in the absence of extracellular Ca^{2+} . The two traces for cytosolic Ca^{2+} represent that of fura-2 (green line) and O-GECO (red line) that were measured simultaneously with mtD1GO-Cam (orange line) and MICU1 FRET (blue dotted trace), respectively.

red-shifted mitochondria targeted cameleon (mtD1GO-Cam) in combination with the near ultra-violet excitable cytosolic Ca^{2+} sensor fura-2 was performed in order to compare the kinetics of cytosolic and mitochondrial Ca^{2+} signals. This approach revealed a lag time (ΔT) of 1.50 ± 0.08 s between the cytosolic Ca^{2+} rise and its transition into the mitochondrial matrix upon intracellular Ca^{2+} mobilization by the IP_3 -generating agonist histamine (Fig. 2A). The molecular mechanism responsible for this temporal shift between rises of $[Ca^{2+}]_{cyto}$ and $[Ca^{2+}]_{mito}$ is so far unknown. To investigate whether or not the Ca^{2+} -dependent de-oligomerization of MICU1 multimers might retard mitochondrial Ca^{2+} signals, identical experiments were performed in cells transfected with siRNA specifically against MICU1. In these MICU1-diminished cells the coupling between cytosolic and mitochondrial Ca^{2+} signals was greatly improved and the mitochondrial Ca^{2+} signal followed almost instantly the cytosolic Ca^{2+} elevation upon histamine stimulation ($\Delta T = 0.93 \pm 0.05$ s) (Fig. 2B,C).

In order to visualize how the temporal pattern of MICU1 de-oligomerization refers to cytosolic Ca^{2+} signals, we imaged dynamic changes of MICU1 FRET simultaneously with cytosolic Ca^{2+} in response to histamine (Fig. 2D). This approach revealed that MICU1 de-oligomerization is only slightly delayed from the histamine-induced increase of $[Ca^{2+}]_{cyto}$ and, thus, clearly precedes mitochondrial Ca^{2+} uptake (Fig. 2E). Notably, app. 90% of the maximal histamine-induced increase of $[Ca^{2+}]_{cyto}$ trigger $\geq 50\%$ of MICU1 de-oligomerization that appears essential to initiate considerable uptake of Ca^{2+} by mitochondria

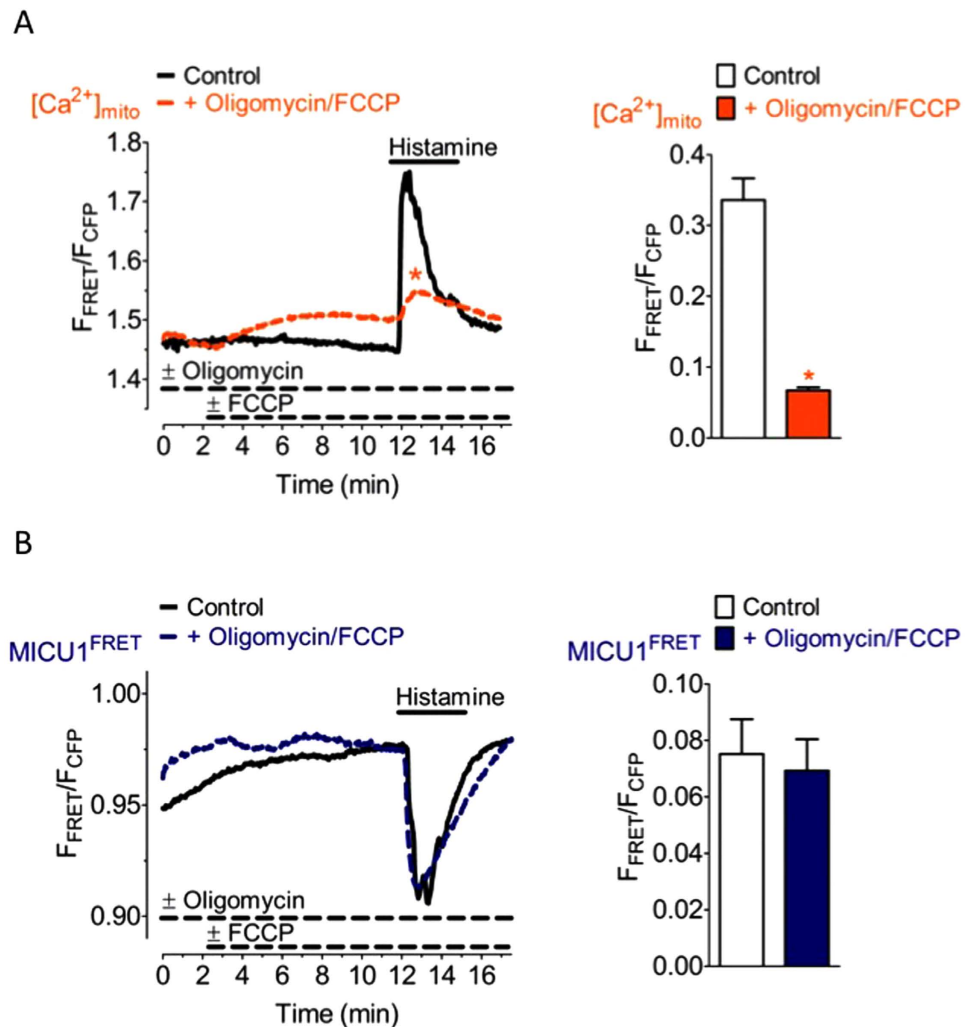


Figure 3. The Ca^{2+} -induced rearrangement of MICU1 multimers is independent of Ψ_{mito} . (A) Average curves reflecting mitochondrial Ca^{2+} signals over time of HeLa cells expressing 4mtD3cpv upon cell treatment with $100\mu M$ histamine in the absence of extracellular Ca^{2+} under control conditions (black curve, $n = 10$) and in the presence of $2\mu M$ oligomycin and $4\mu M$ FCCP (orange curve, $n = 14$). Bar graph shows respective maximal Δ ratio signals; mean \pm SEM. * $P < 0.05$ vs. control. (B) Average MICU1 FRET ratio signals of HeLa cells co-expressing MICU1-CFP and MICU1-YFP in response to $100\mu M$ histamine in Ca^{2+} -free conditions in the absence of oligomycin and FCCP (control, black curve, $n = 3$) and the presence of $2\mu M$ oligomycin and $4\mu M$ FCCP (blue curve, $n = 6$). Bar graph shows respective maximal Δ MICU1 FRET ratio signals; mean \pm SEM.

(Fig. 2D,E). These data dissect the transfer of cytosolic Ca^{2+} into mitochondria into (at least) four sequential steps: (i) cytosolic Ca^{2+} elevation and transfer into the intermembrane space, (ii) binding of Ca^{2+} to MICU1 oligomers, (iii) MICU1 de-oligomerization, and (IV) activation of the MCU.

Rearrangement of MICU1 multimers occurs independently of the mitochondrial membrane potential and matrix Ca^{2+} elevation. In order to test if the mitochondrial membrane potential (Ψ_{mito}) impacts rearrangement of MICU1 multimers, cells were treated with oligomycin and the uncoupling agent carbonyl cyanide-4-(trifluoromethoxy) phenylhydrazone (FCCP) to efficiently depolarize mitochondria¹², thus, only very small mitochondrial Ca^{2+} signals in response to histamine were observed (Fig. 3A) approving the loss of Ψ_{mito} under these conditions. However, depolarization of mitochondria did neither affect basal MICU1 FRET nor the histamine-triggered reduction of the inter-MICU1 FRET signal (Fig. 3B). These data indicate that the rearrangement of MICU1 multimers upon intracellular Ca^{2+} mobilization with an IP_3 -generating agonist occurs independently of Ψ_{mito} and the mitochondrial matrix Ca^{2+} elevation.

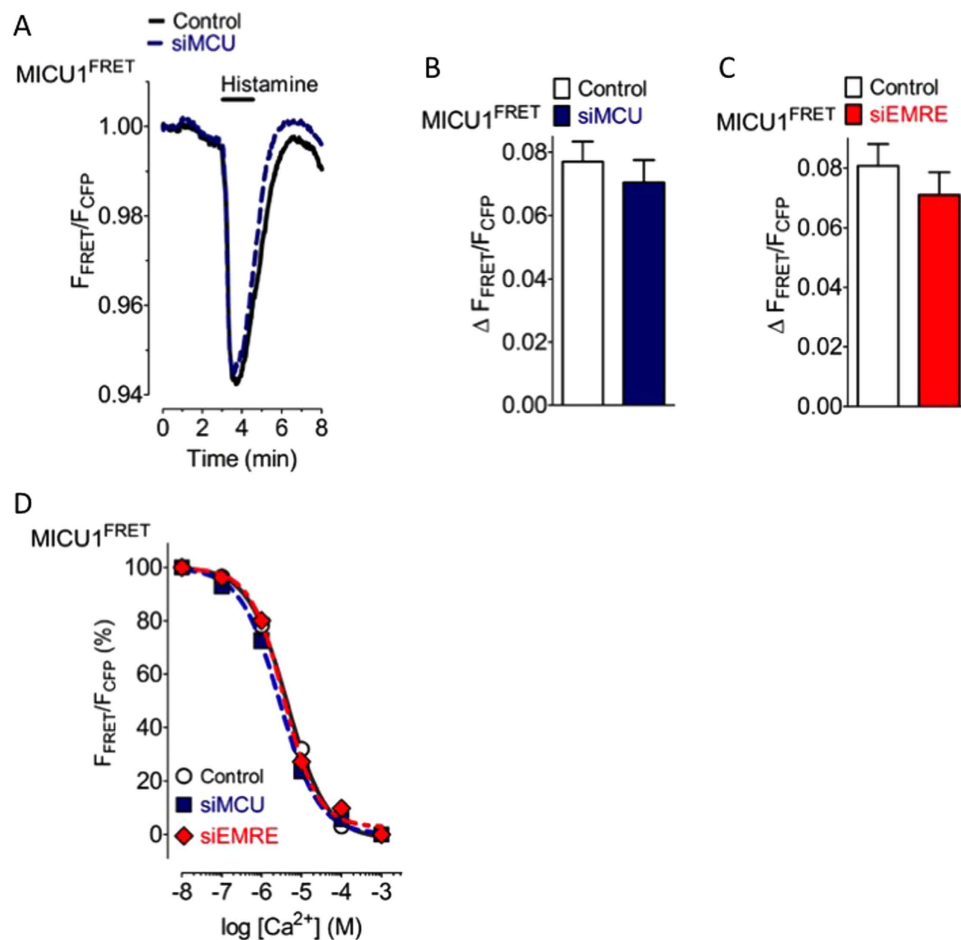


Figure 4. The Ca²⁺-induced rearrangement of MICU1 multimers is independent of the expression level of MCU and EMRE. (A) Average curves of MICU1 FRET ratio signals over time in response to 100 μM histamine in Ca²⁺-free solution of control HeLa cells (black curve, n = 23) and cells treated with siRNA against MCU (blue curve, n = 22). (B) Bars represent maximal Δ MICU1 FRET ratio values (mean ± SEM) extracted from curves shown in panel A. (C) Bars represent maximal Δ MICU1 FRET ratio values upon cell treatment with 100 μM histamine in Ca²⁺-free solution of control HeLa cells (white column, n = 19) and cells treated with siRNA against EMRE (red column, n = 12). (D) Concentration response curves showing the effects of different Ca²⁺ concentrations on the MICU1 FRET ratio in ionomycin- (3 μM) treated control HeLa cells (black curve, white circles, n = 7–9), cells reduced of MCU (blue dotted curve, blue filled squares, n = 8–10), and cells reduced of EMRE (red dotted curve, red filled rhombs, n = 10).

MICU1 multimers rearrange irrespective of the expression level of MCU and EMRE. MICU1 is known to interact with EMRE¹⁶ that represents the second pore forming protein of the mitochondrial Ca²⁺ complex beside MCU^{28–30}, which is regulated by MICU1^{19,21,25}. To investigate the importance of EMRE and MCU for the Ca²⁺-triggered rearrangement of MICU1 multimers, expression of either EMRE or MCU were diminished by respective verified siRNAs (Supplementary Fig. 9). Diminution of the expression of either MCU or EMRE strongly reduced mitochondrial Ca²⁺ uptake (Supplementary Fig. 10) while no effect on cytosolic Ca²⁺ signaling was observed (Supplementary Fig. 11). However, the rearrangement of the MICU1 multimers upon stimulation with histamine was neither affected by knock-down of MCU (Fig. 4A,B) nor EMRE (Fig. 4C). In line with these findings the EC₅₀ of Ca²⁺ to reduce the inter-MICU1 FRET signal remained unaffected in cells diminished of either MCU or EMRE (Fig. 4D).

Discussion

The present study describes the dynamics of MICU1 (re-)organization in response to cytosolic Ca²⁺ elevations in intact cells. Using the FRET technology we could correlate the Ca²⁺ induced rearrangement of MICU1 multimers with the activation of mitochondrial Ca²⁺ uniport and examined the impact of mitochondrial Ca²⁺, Ψ_{mito} and the expression levels of MCU and EMRE for MICU1 (re-)organization. Our data highlight that an elevation of cytosolic free Ca²⁺ rearranges MICU1 multimers to smaller complexes in intact cells. These findings are consistent with a recent report showing that recombinant

Ca²⁺-free MICU1 exists as hexamer and rearranges in the presence of Ca²⁺ to dimers^{7,23}. Hence, our data that point to the existence of large MICU1 complexes that suppresses mitochondrial Ca²⁺ uptake at low cytosolic Ca²⁺ is in line with previous reports about the inactivity of MCU under resting conditions^{8,18}.

Our approach of live-cell monitoring the inter-MICU1 FRET allows the visualization of MICU1 (re-)organization within the intact cell in life-time. Notably, calculation of the changes in MICU1 FRET probability in the transition from hexamers to dimers revealed a theoretically achievable reduction of FRET by app. 52% (Supplementary Information, Supplementary Fig. 12). However, the actual measured changes in FRET upon MICU1 rearrangement triggered by histamine was app. 7%. The discrepancy between the theoretical FRET changes upon the rearrangement of hexamers to independent dimers and the actual measured one might be due to basically two reasons: *first*, the high expression of FP tagged MICU1 proteins might result in lower oligomerization states, and *second*, upon histamine-induced intracellular Ca²⁺ release, MICU1 de-oligomerization most likely occurs predominantly within the junctions between the ER and mitochondria where high Ca²⁺ gradients are developed²⁷, thus, only a small portion of MICU1 hexamers actually undergoes rearrangement under this conditions. This assumption is further supported by the app. 15% FRET reduction achieved in the assessment of the concentration response curve of MICU1 FRET dynamic to Ca²⁺.

Our approach that allowed correlation of the kinetics of MICU1 (re-)organization with cellular Ca²⁺ dynamics data revealed that the rearrangement of MICU1 multimers by cytosolic Ca²⁺ strictly correlates with the cytosolic Ca²⁺ concentration and is rapidly reversible. The *in situ* calibration indicates that the rearrangement of MICU1 senses Ca²⁺ changes in the range between the low basal Ca²⁺ levels of 100 nM up to 100 μM. With an EC₅₀ of around 4 μM, the Ca²⁺ sensitivity of MICU1 rearrangement lays exactly in the range of Ca²⁺ hot spots (3.78 and 16.4 μM) that have been measured at the outer mitochondrial membrane between the junction of mitochondria and the ER²⁷. In line with this report, the IP₃-mediated intracellular Ca²⁺ mobilization almost instantly yielded MICU1 rearrangement, while Ca²⁺ entry via the store-operated Ca²⁺ entry pathway^{31,32} triggered only a slow and moderate re-organization of MICU1 multimers. These differences between the MICU1 rearrangement upon intracellular Ca²⁺ release and entering Ca²⁺ are consistent with previous reports that described a rather slow on-kinetics of entering Ca²⁺ at the mitochondrial surface without the formation of Ca²⁺ hot spots and slow mitochondrial Ca²⁺ accumulation^{14,27,33}.

Similar to entering Ca²⁺, the inhibition of SERCA by BHQ yielded only slow and small rearrangement of MICU1 multimers and, thus, explains the marginal effect of SERCA inhibition on mitochondrial Ca²⁺ uptake. Since the diminution of MICU1 expression substantially gains mitochondrial Ca²⁺ uptake in response to intracellular Ca²⁺ release by SERCA inhibition, the prominent role of MICU1 as a negative regulator of mitochondrial Ca²⁺ uniport is clearly demonstrated. This assumption is further supported by our experiments in which cytosolic and mitochondrial free Ca²⁺ were simultaneously measured and the lag time of app. 1.5 s between cytosolic Ca²⁺ elevation and the mitochondrial Ca²⁺ uptake was strongly reduced in cells with diminished expression of MICU1. Hence, the correlation between cytosolic Ca²⁺ elevation, the rearrangement of MICU1 multimers and mitochondrial Ca²⁺ signals, revealed that MICU1 reorganization temporally occurs in between the Ca²⁺ rise within the two compartments. Notably, significant mitochondrial Ca²⁺ uptake appears to occur at app. 50% rearrangement of MICU1 multimers. These data demonstrate that for activation of the MCU/EMRE complex to achieve mitochondrial Ca²⁺ influx, app. 50% of the MICU1 multimers have to be rearranged. Although these findings might be due to the overexpression of MICU1 in our model, the MICU1-dependent lack of mitochondrial Ca²⁺ uptake in response to SERCA inhibition supports this assumption.

Mitochondrial Ca²⁺ uptake strongly depends on Ψ_{mito} that establishes the driving force for Ca²⁺ uniport into the organelle. However, whether or not Ψ_{mito} also impacts on MICU1 organization has not been investigated so far. Our data with completely depolarized mitochondria revealed an unchanged MICU1 dynamics despite a greatly reduced mitochondrial Ca²⁺ uptake. These data demonstrate that neither Ψ_{mito} nor matrix Ca²⁺ are involved in the rearrangement of MICU1 complexes and confirms cytosolic Ca²⁺ as possible the sole regulator of MICU1 (re-)organization²³.

Considering the interaction of MICU1 with EMRE and MCU^{7,16,18,19,23,25,29}, the importance of these two pore-forming proteins^{16,28,29} for the structural organization of MICU1 was evaluated. Although the siRNA-mediated diminution of either of these proteins resulted in strongly reduced mitochondrial Ca²⁺ uptake, the Ca²⁺-triggered rearrangement of MICU1 multimers, their arrangement upon the reduction of cytosolic Ca²⁺ to basal levels, and the sensitivity to cytosolic Ca²⁺ remained unaffected by the reduction of MCU or EMRE. These data demonstrate that the structural (re-)organization of MICU1 upon elevation of cytosolic free Ca²⁺ does not involve MCU or EMRE indicating that the Ca²⁺-induced rearrangement of MICU1 multimers is a robust process that does most likely not require other interaction partners.

Despite the topology of MICU1 is still under debate^{18,21,25,30}, our data that, *first*, MICU1 FRET rearrangement follows cytosolic but not matrix mitochondrial Ca²⁺, *second*, MICU1 knockdown results in a faster mitochondrial Ca²⁺ uptake, *third*, rearrangement of MICU1 FRET precedes mitochondrial Ca²⁺ uptake, *forth*, MICU1 FRET is independent from Ψ_{mito} , and *fifth*, neither knockdown of MCU nor of EMRE influences MICU1 FRET rearrangement indicate that MICU1 anchors with its N-terminus in the IMM while the core protein is oriented towards intermembrane space and not to the matrix.

Our results provide new mechanistic insights in the regulation of mitochondrial Ca^{2+} uptake. For the first time, the kinetics and adjustments of one of the most important molecular gatekeeper of mitochondrial Ca^{2+} uptake was visualized in intact cells. Our data revealed cytosolic Ca^{2+} as the most prominent regulator of the structural organization of MICU1, which in the form of a homo-multimere potently inhibits the MCU/EMRE mitochondrial Ca^{2+} channel complex. Moreover, neither Ψ_{mito} nor matrix Ca^{2+} , nor MCU or EMRE were found to affect the Ca^{2+} -controlled (dis)assembly of MICU1 multimers. Finally, our data provide important details for a better understanding of the molecular regulation of an intricate mitochondrial Ca^{2+} uptake machinery.

Methods

Chemicals and Buffers. All reagents and chemicals for buffers and solutions were obtained from Carl Roth (Karlsruhe, Germany). Fura-2/AM was obtained from Teflabs (Texas Fluorescence Labs Inc., Austin, Texas, USA). BHQ and histamine were purchased from Sigma-Aldrich (Vienna, Austria). FCCP and oligomycin were from Abcam Biochemicals (Cambridge, UK). Prior to experiments HeLa cells were stored and loaded with fura-2/AM in a buffer composed of (in mM): 2 CaCl_2 , 135 NaCl, 5 KCl, 1 MgCl_2 , 1 HEPES, 2.6 NaHCO_3 , 0.44 KH_2PO_4 , 0.34 Na_2HPO_4 , 10 D-glucose, 0.1% vitamins, 0.2% essential amino acids and 1% penicillin/streptomycin pH 7.4. For Ca^{2+} measurements HeLa cells were perfused in a HEPES buffered solution containing (in mM): 2 CaCl_2 , 140 NaCl, 5 KCl, 1 MgCl_2 , 1 HEPES and 10 D-Glucose pH 7.4. To achieve a nominal Ca^{2+} free environment either 1 mM EGTA was added instead of 2 mM CaCl_2 . For Kd determination of MICU1 FRET we used the same buffer containing 3 mM EGTA supplemented with 3–10 μM ionomycin (Abcam Biochemicals, Cambridge, UK) and CaCl_2 was added according to the CaBuff software (G. Droogmans, Fysiologie, Leuven) to obtain buffer solutions of 0.1, 1, 10, 100 and 1000 μM free Ca^{2+} concentrations.

Cell culture and transfection. HeLa cells at passage >50 were cultured on glass cover slips ($\varnothing = 30$ mm) using DMEM (Sigma-Aldrich, Vienna, Austria) containing 10% FCS (PAA, Pasching, Austria), penicillin (100 U/ml) and streptomycin (100 U/ml) in a humidified incubator (37 °C, 5% CO_2 /95% air). 2–3 days prior experiments HeLa cells were transfected in DMEM (without FCS and antibiotics) with plasmids (1–4 $\mu\text{g}/\text{ml}$ total) and/or siRNA (100 nM) using 4 $\mu\text{g}/\text{ml}$ TransFast™ transfection reagent (Promega, Madison, WI, USA).

Plasmids and siRNAs. For engineering MICU1-CFP and MICU1-YFP the coding sequence (cds) of human MICU1 (hMICU1, NM_006077.3) without a stop codon was amplified from a HeLa cDNA by PCR using primers (Invitrogen, Vienna, Austria): forward: 5'-ACGGATCCACCATGTTTCGTCTGAACTCAC-3' and reverse: 5'-ACGAATTCCTGTTTGGGTAAAGCGAAGTCC-3'. The PCR fragment was cloned in a pcDNA3.1 (+) vector via BamHI and EcoRI sites. The cds of either enhanced cyan fluorescent protein (CFP) or citrine (YFP) were amplified with the same primers: forward: 5'-AAGAATTCATGGTGAGCAAGGGCGAGGAG-3' and reverse: 5'-CCTCTAGAACTTGTACAGCTCGTCCATGC-3' and each C-terminally fused to hMICU1 using the EcoRI and XbaI sites. EF hand mutated MICU1 and O-GECO1 constructs were purchased from Addgene (Cambridge, MA, USA). The EF hand mutated MICU1 (EFmut) was amplified using the same primers as described above and C-terminally fused with either ECFP or Citrine like the wild-type MICU1. A mitochondrial targeted mtO-GECO1 was generated upon PCR amplification of O-GECO1 using the forward primer 5'-AACTCGAGTATGGTTCGACTCATCACGTCG-3' and a reverse primer 5'-GCAAGCTTTTACTTCGCTGTCATCAT-3' and the PCR fragment was N-terminally fused with the mitochondrial targeting sequence (4mt) via XhoI and HindIII restriction sites in a pcDNA3.1(-) vector. 4mtD1GO-Cam was constructed as previously described³⁴ and 4mtD3cpV (Mt-cameleon-pcDNA3) was a gift from Prof. Dr. Roger Tsien. For silencing hMCU (NM_138357.2), hEMRE (NM_033318.4) or hMICU1 we used siRNAs from Microsynth (Balgach, Switzerland) with following sequences (sense strands, 5'-3'): hMCU-si1 (GCCAGAGACAGACAAUACU), hMCU-si2 (GGAAAGGGAGCUUAUUGAA); hEMRE-si (GAACUUUGCUGCUCUACUU); hMICU1-si1 (GCAGCUCAAGAAGCACUCAA), hMICU1-si2 (GCAAUGGCGAACUGAGCAAUA) or 3'UTR-siMICU1 (AGAAGUCUGUGAUGAUAAA, binds in the non-coding 3' terminal untranslated region of MICU1); and a scrambled negative control-si (UUCUCCGAACGUGUCACGU).

Quantitative reverse transcription PCR. To determine hEMRE and hMCU silencing HeLa cells were transiently transfected with the respective siRNA(s). The PEQLAB total RNA isolation kit (PEQLAB Biotechnologie GmbH, Erlangen, Germany) was used for total RNA isolation and 1 μg of each RNA sample were reverse transcribed with a cDNA synthesis kit (Applied Biosystems, USA). The efficiency of siRNA mediated knockdown was validated by real time PCR on a LightCycler 480 (Roche Diagnostics, Vienna, Austria). Target genes and human GAPDH (no. QT01192646, QuantiTect® Primer Assay, Qiagen, Hilden, Germany) as housekeeping gene were amplified within the respective cDNA samples using the GoTaq® qPCR Master Mix (Promega) and specific real time primer pairs (Invitrogen): hMCU forward: 5'-TTCCTGGCAGAATTTGGGAG-3', hMCU reverse: 5'-AGAGATAGGCTTGAGTGTGAAC-3'; hEMRE forward: 5'-TCGCTGGCTAGTATTGGCAC-3', hEMRE reverse: 5'-GGAGAAGGCCGAAGGACATT-3'. Relative expression of the hEMRE and hMCU

were normalized to GAPDH expression and data were analyzed by the REST software (Qiagen, Hilden, Germany).

Fluorescence microscopy. Ca^{2+} imaging and dynamic FRET measurements between MICU1-CFP and MICU1-YFP were performed on an inverted microscope (Axio Observer.A1, Zeiss, Göttingen, Germany) equipped with a polychromator illumination system (VisiChrome, Visitron Systems, Puchheim, Germany) and a thermoelectric-cooled CCD camera (Photometrics CoolSNAP HQ, Visitron Systems). Cells were imaged with a 40 \times oil-immersion objective (Zeiss). Fura-2 and the 4mtD1GO-Cam were alternately excited at 340 nm or 380 nm and at 477 nm, respectively, with an ultra-fast switching monochromator, the Polychrome V (Till Photonics), equipped with an excitation filter (E500spuv) and a dichroic filter (495dcxr, Chroma Technology Corp., VT). Emitted light was simultaneously collected at 510 nm (Fura-2 and GFP of GO-Cam) and at 600 nm (FRET-channel of GO-Cam) using a single beam splitter design (Dichrotome, Till Photonics) that was equipped with a dual band emission filter (59004m ET Fitc/Tritc Dual Emitter) and a second dichroic filter (560dcxr, Chroma Technology Corp.). Images were recorded with a CCD camera (AVT Stringray F145B, Till Photonics). The digital imaging system was controlled by the live-acquisition software v2.0.0.12 (Till Photonics), as described previously³⁴. Dual recordings of MICU1 FRET and $[\text{Ca}^{2+}]_{\text{cyto}}$ was performed in HeLa cells co-transfected with MICU1-CFP, MICU1-YFP and O-GECO1 or mtO-GECO1, respectively. MICU1-CFP and (mt)O-GECO1 were alternately illuminated at 430 nm and 575 nm, respectively, in single individual cells. Emitted light was collected at 535 nm for MICU1 FRET and 610 nm for (mt)O-GECO1 using the XF56 filter set of Omega Optical.

Statistics. All experiments were repeated at least three times on two different days. Data from multiple experiments were quantified to determine absolute or percent changes, expressed as mean \pm SEM where n reflects the actual number of repeats. Statistical analyses were performed with unpaired Student's t-test. When not normally distributed, a Mann-Whitney U test was applied. Differences in means among multiple data sets were analyzed by using one-way analysis of variance (ANOVA) and subsequent Bonferroni *post hoc* test and two-tailed Student's t-test. $P < 0.05$ was considered significant. Data were analyzed either with MS Excel 2011 or with Graphpad Prism version 5.0.

References

1. Szabadkai, G., Pitter, J. & Spät, A. Cytoplasmic Ca^{2+} at low submicromolar concentration stimulates mitochondrial metabolism in rat luteal cells. *Pflügers Arch* **441**, 678–685 (2001).
2. Malli, R. & Graier, W. F. Mitochondrial Ca^{2+} channels: Great unknowns with important functions. *FEBS Lett* **584**, 1942–1947 (2010).
3. Szabadkai, G. & Duchen, M. R. Mitochondria: the hub of cellular Ca^{2+} signaling. *Physiology (Bethesda)* **23**, 84–94 (2008).
4. Duchen, M. R., Verkhatsky, A. & Muallem, S. Mitochondria and calcium in health and disease. *Cell Calcium* **44**, 1–5 (2008).
5. Baughman, J. M. *et al.* Integrative genomics identifies MCU as an essential component of the mitochondrial calcium uniporter. *Nature* **476**, 341–345 (2011).
6. De Stefani, D., Raffaello, A., Teardo, E., Szabò, I. & Rizzuto, R. A forty-kilodalton protein of the inner membrane is the mitochondrial calcium uniporter. *Nature* **476**, 336–340 (2011).
7. Wang, L., Yang, X. & Shen, Y. Molecular mechanism of mitochondrial calcium uptake. *Cell Mol. Life Sci.* **72**, 1489–1498 (2015).
8. Mallilankaraman, K. *et al.* MCUR1 is an essential component of mitochondrial Ca^{2+} uptake that regulates cellular metabolism. *Nat. Cell Biol.* **14**, 1336–1343 (2012).
9. Jiang, D., Zhao, L. & Clapham, D. E. Genome-Wide RNAi Screen Identifies Letm1 as a Mitochondrial $\text{Ca}^{2+}/\text{H}^{+}$ Antiporter. *Science* **326**, 144–147 (2009).
10. Waldeck-Weiermair, M. *et al.* The leucine zipper EF hand-containing transmembrane protein 1 (LETM1) and uncoupling proteins- 2 and 3 (UCP2/3) contribute to two distinct mitochondrial Ca^{2+} uptake pathways. *J. Biol. Chem.* **286**, 28444–28455 (2011).
11. Waldeck-Weiermair, M. *et al.* Molecularly distinct routes of mitochondrial Ca^{2+} Uptake are activated depending on the activity of the sarco/endoplasmic reticulum Ca^{2+} ATPase (SERCA). *J. Biol. Chem.* **288**, 15367–15379 (2013).
12. Trenker, M., Malli, R., Fertschai, I., Levak-Frank, S. & Graier, W. F. Uncoupling proteins 2 and 3 are fundamental for mitochondrial Ca^{2+} uniport. *Nat. Cell Biol.* **9**, 445–452 (2007).
13. Trenker, M., Fertschai, I., Malli, R. & Graier, W. F. UCP2/3 — likely to be fundamental for mitochondrial Ca^{2+} uniport. *Nat. Cell Biol.* **10**, 1237–1240 (2008).
14. Waldeck-Weiermair, M. *et al.* The contribution of UCP2 and UCP3 to mitochondrial Ca^{2+} uptake is differentially determined by the source of supplied Ca^{2+} . *Cell Calcium* **47**, 433–440 (2010).
15. Raffaello, A. *et al.* The mitochondrial calcium uniporter is a multimer that can include a dominant-negative pore-forming subunit. *EMBO J.* **32**, 2362–2376 (2013).
16. Sancak, Y. *et al.* EMRE is an essential component of the mitochondrial calcium uniporter complex. *Science* **342**, 1379–1382 (2013).
17. Perocchi, F. *et al.* MICU1 encodes a mitochondrial EF hand protein required for Ca^{2+} uptake. *Nature* **467**, 291–296 (2010).
18. Csordás, G. *et al.* MICU1 controls both the threshold and cooperative activation of the mitochondrial Ca^{2+} Uniporter. *Cell Metab.* **17**, 976–987 (2013).
19. Patron, M. *et al.* MICU1 and MICU2 finely tune the mitochondrial Ca^{2+} uniporter by exerting opposite effects on MCU activity. *Mol. Cell.* **53**, 726–737 (2014).
20. Plovanich, M. *et al.* MICU2, a paralog of MICU1, resides within the mitochondrial uniporter complex to regulate calcium handling. *PLoS ONE* **8**, e55785 (2013).

21. Hoffman, N. E. *et al.* MICU1 motifs define mitochondrial calcium uniporter binding and activity. *Cell Reports* **5**, 1576–1588 (2013).
22. Gifford, J. L., Walsh, M. P. & Vogel, H. J. Structures and metal-ion-binding properties of the Ca²⁺-binding helix-loop-helix EF-hand motifs. *Biochem J* **405**, 199–221 (2007).
23. Wang, L. *et al.* Structural and mechanistic insights into MICU1 regulation of mitochondrial calcium uptake. *EMBO J.* **33**, 594–604 (2014).
24. Mallilankaraman, K. *et al.* MICU1 is an essential gatekeeper for MCU-mediated mitochondrial Ca²⁺ uptake that regulates cell survival. *Cell* **151**, 630–644 (2012).
25. Foskett, K. J. & Madesh, M. Regulation of the mitochondrial Ca²⁺ uniporter by MICU1 and MICU2. *Biochem. Biophys. Res. Commun.* **449**, 377–383 (2014).
26. Osibow, K., Malli, R., Kostner, G. M. & Graier, W. F. A new type of non-Ca²⁺-buffering Apo(a)-based fluorescent indicator for intraluminal Ca²⁺ in the endoplasmic reticulum. *J. Biol. Chem.* **281**, 5017–5025 (2006).
27. Giacomello, M. *et al.* Ca²⁺ hot spots on the mitochondrial surface are generated by Ca²⁺ mobilization from stores, but not by activation of store-operated Ca²⁺ channels. *Mol. Cell* **38**, 280–290 (2010).
28. Foskett, K. J. & Philipson, B. The mitochondrial Ca²⁺ uniporter complex. *J. Mol. Cell. Cardiol.* **78**, 3–8 (2015).
29. De Stefani, D. & Rizzuto, R. Molecular control of mitochondrial calcium uptake. *Biochem. Biophys. Res. Commun.* **449**, 373–376 (2014).
30. Kamer, K. J., Sancak, Y. & Mootha, V. K. The uniporter: From newly identified parts to function. *Biochem. Biophys. Res. Commun.* **449**, 370–372 (2014).
31. Putney, J. W. J. A model for receptor-regulated calcium entry. *Cell Calcium* **7**, 1–12 (1986).
32. Parekh, A. B. Store-operated Ca²⁺ entry: dynamic interplay between endoplasmic reticulum, mitochondria and plasma membrane. *J. Physiol.* **547**, 333–348 (2003).
33. Waldeck-Weiermair, M. *et al.* Uncoupling protein 3 adjusts mitochondrial Ca²⁺ uptake to high and low Ca²⁺ signals. *Cell Calcium* **48**, 288–301 (2010).
34. Waldeck-Weiermair, M. *et al.* Spatiotemporal correlations between cytosolic and mitochondrial Ca²⁺ signals using a novel red-shifted mitochondrial targeted cameleon. *PLoS ONE* **7**, e45917 (2012).

Acknowledgements

We thank Sandra Blass for her excellent technical assistance and Prof. Dr. Roger Tsien, University of California San Diego, CA, USA for providing us the 4mtD3cpV (mt-cameleon-pcDNA3). This work was funded by the Austrian Science Funds (FWF, DKplus W 1226-B18). W.P. is supported by the Austrian Academic Exchange Services (ÖAD) and is a doctoral fellow of the doctoral school Molecular Medicine at the Medical University of Graz. B.G., C.T. and C.K. are supported by BioTechMed (B.G.) or the FWF (C.T.M.-S. & C.K.) or as doctoral fellows within the doctoral program Metabolic and Cardiovascular Disease (FWF, DKplus W 1226-B18) at the Medical University of Graz. Microscopic equipment is part of the Nikon-Center of Excellence, Graz that is supported by the Austrian infrastructure program (HRSM 2013/2014), Nikon Austria Inc. and BioTechMed.

Author Contributions

W.P., M.W.-W. and C.T.M.-S. performed experiments, B.G. calculated FRET efficiencies and evaluated FRET experiments, C.K. and R.R. cloned the respective constructs and cultivated the cells. R.M. analyzed the data and together with W.F.G. designed this study and wrote the manuscript.

Additional Information

Supplementary information accompanies this paper at <http://www.nature.com/srep>

Competing financial interests: The authors declare no competing financial interests.

How to cite this article: Waldeck-Weiermair, M. *et al.* Rearrangement of MICU1 multimers for activation of MCU is solely controlled by cytosolic Ca²⁺. *Sci. Rep.* **5**, 15602; doi: 10.1038/srep15602 (2015).



This work is licensed under a Creative Commons Attribution 4.0 International License. The images or other third party material in this article are included in the article's Creative Commons license, unless indicated otherwise in the credit line; if the material is not included under the Creative Commons license, users will need to obtain permission from the license holder to reproduce the material. To view a copy of this license, visit <http://creativecommons.org/licenses/by/4.0/>